PCCP

Accepted Manuscript

ROYAL SOCIETY OF CHEMISTRY

www.rsc.org/pccp

Catalyzed Hydrogen Sorption Mechanism in Alkali Alanates

Züleyha Özlem Kocabas Atakli,[a] Elsa Callini, [a,b] Shunsuke Kato, [a,b] Philippe Mauron,[a,b] Shin-Ichi Orimo,[c] and Andreas Züttel[a,b*]

[a] EMPA, Swiss Federal Laboratories for Materials Science and Technology, CH-8600 Dübendorf, Switzerland

[b] Ecole polytechnique fédérale de Lausanne (EPFL), Institut des sciences et ingénierie chimiques, CH-1015 Lausanne, Switzerland

[c] Institute for Materials Research, Tohoku University, Sendai 980-8577, Japan

Abstract: The hydrogen sorption pathways of alkali alanates were analyzed and a mechanism for the catalytic hydrogen sorption was developed. Gibbs free energy values of selected intermediate steps were calculated based on experimentally determined thermodynamic data (enthalpies and entropies) of individual hydrides: $MAlH_4$, M_3AlH_6, and MH. The values of the activation energies, based on the intermediates M^+, H^-, MH, and AlH_3, were obtained. The mechanism of the catalytic activity of Ti is finally clarified: we present an atomistic model, where $MAlH_4$ desorbs hydrogen through the intermediates M^+, H^-, MH, and AlH_3 to the hexahydride M_3AlH_6 and finally the elemental hydride MH. The catalyst acts as a bridge to transfer the M^+ and H^- from $MAlH_4^-$ to the neighboring AlH_4^-, forming AlH_6^{3-} and finally isolated MH, leaving AlH_3 behind, which spontaneously desorbs hydrogen to give Al and 1.5 H_2. The proposed mechanism is symmetric in the direction of hydrogen desorption as well as readsorption processes.

* Author to whom correspondence should be addressed
andreas.zuettel@empa.ch , Tel: +41 58 765 40 38

1. Introduction

While the volumetric hydrogen density in hydrides reaches twice the density of liquid hydrogen, the gravimetric hydrogen density in metal hydrides is limited to about 2.5 mass%. Since Bogdanovic and co-workers[1] presented Ti-catalyzed hydrogen sorption in sodium alanate ($NaAlH_4$) at the MH1996 conference, the complex hydrides have been intensively investigated for solid phase hydrogen storage. $NaAlH_4$ desorbs hydrogen in three distinct steps, where Na_3AlH_6 and NaH are intermediate products of the partially dehydrogenated alanate in the process as shown by the following three reactions:

$$3NaAlH_4 \rightarrow Na_3AlH_6 + 2Al + 3H_2 \rightarrow 3NaH + 3Al + \frac{9}{2}H_2 \rightarrow 3Na + 3Al + 6H_2 \qquad (1)$$

From the total amount of hydrogen (7.4 mass%) in $NaAlH_4$, half of the hydrogen, that is, 3.7 mass%, is desorbed in the first reaction at 353 K ($p(H_2)$ = 0.1 MPa), one quarter, that is, 1.85 mass%, is desorbed in the second reaction at 423 K ($p(H_2)$ = 0.1 MPa), and one quarter, that is, 1.85 mass%, is desorbed in the third reaction at 700 K ($p(H_2)$ = 0.1 MPa).[2] A two-step decomposition reaction of $NaAlH_4$ was proposed by Balema and Balema[3] due to the absence of Na_3AlH_6 species. They proposed that NaH obtained from the direct decomposition reaction of $NaAlH_4$ could react with the remaining $NaAlH_4$ in order to produce the Na_3AlH_6 as indicated in the following:

$$NaAlH_4 \rightarrow NaH + AlH_3 \qquad (2)$$

$$NaAlH_4 + 2NaH \rightarrow Na_3AlH_6 \qquad (3)$$

In the neat $NaAlH_4$ system, the activation energies for the first and second dehydrogenation reactions shown in Reaction (1) are 118 and 124 kJ/mol H_2, respectively.[4] Adding a few molar percent of $TiCl_3$ to the $NaAlH_4$ reduces the activation energies to 80 and 96 kJ/mol H_2, and the isotherm of the reabsorption of hydrogen follows the desorption isotherm with almost no hysteresis.[1,5,6] The role of the Ti as a catalyst is to increase the reaction rate for the hydrogen desorption and absorption reaction, that is, to allow the reaction to equilibrate in the time frame of the experiment.[7] A few molar percent of $TiCl_3$ have been added to $NaAlH_4$ by

ball milling or in a solvent.[1,8,9] Other Ti salts and Ti compounds, such as TiF_3, $Ti(OBu)_4$, TiH_2, and TiO_2, have also been well studied and it was found that the anion reacts with the sodium in the alanate. [10,11,12,13,14] The added quantity of the Ti salt affects the increase of the reaction rate; that is, up to 5 mol%, a linear increase of the reaction rate as a function of the added amount was found, while for larger quantities the reaction rate did not increase anymore.[5] Apart from that, Bogdanovic et al.[15] reported that adding 2 mol% of $ScCl_3$ and $CeCl_3$ into $NaAlH_4$ reduces hydrogenation times by a factor of approximately two at high pressure and by a factor of ten at low pressure in contrast to adding $TiCl_3$. Wang et al.[16] compared the reversible hydrogen storage properties of Sc-$NaAlH_4$ with those of Ti-$NaAlH_4$. They concluded that Sc-$NaAlH_4$ cycled better than Ti-$NaAlH_4$ and that Sc-doped $NaAlH_4$ exhibited comparable or, in some cases, even higher hydrogen storage capacities than Ti-$NaAlH_4$. Other metals like Pd, Pt, Ir, Rh, and Ru that are commonly used as hydrogenation catalyst elements have an insignificant effect on the hydrogenation cycling[7].

The following questions come to mind: 1) What is the catalytically active material? 2) Which are the catalytically active sites? 3) In which oxidation state is the catalyst? 4) What is the mechanism of the catalyzed reaction? Despite years of intense investigations of a large variety of catalytic materials added to alanates, the mechanism of the catalyzed reactions including the role of the catalyst remains unresolved.

Different ideas to explain the mechanisms of the Ti-catalyzed reactions have been proposed by several authors and will be briefly reviewed in the following. One of the early studies by Ivanov[17] on Ti as a catalyst in $MAlH_4$ explains the role of the Ti species on or in the surface layer to provide a barrierless path for the hydrogen dissociation/recombination ($H_2 \rightleftarrows 2H$) reaction as behaving as a “hydrogen pump”. Hydrogen atoms diffuse to and from the reaction center independently. However, there are various metals that are known to show a very low dissociation barrier for hydrogen, for example, Pd and Pt, which do not increase the reaction rate of the hydrogen desorption from alanates similarly to Ti. Furthermore, there are no quasi-free hydrogen atoms in alanates but rather hydrogen carrying at least a partial negative charge. Gunaydin et al.[18] proposed a vacancy-mediated mechanism that includes initiation of the formation of mobile AlH_3 and NaH vacancies at the phase boundaries of Al-$NaAlH_4$ and $NaAlH_4$-Na_3AlH_6. They found that H_2 evolved at the Al-$NaAlH_4$ interface. Borgschulte et al.[19] further support this vacancy-diffusion-limited interfacial mechanism by suggesting that the role

of Ti in the system is to act as a shuttle at the interface of Al-$NaAlH_4$. However the decomposition of Na_3AlH_6 was not considered along with the reason for the formation of such an interface in these proposed mechanisms. Since the hydrogen desorption occurs at the surface, the interface is moving through the alanate crystal and therefore no transport limitation is present. The desorption products are formed at the surface and subsequently diffuse to each other to form bulk materials. Recently, Peles and van de Walle[20] demonstrated that the presence of Ti could change the Fermi level of the crystal and therefore the energy required to create a charged hydrogen defect decreased. Sun et al.[21] and Singh et al.[22] suggest that during decomposition of $NaAlH_4$, Ti particles are the centers for nucleation and growth of the decomposed phases. However, the growth of the product phases is not directly connected to the hydrogen release and the nucleation of the phases does not explain the catalytic activity of the reabsorption reaction. Sandrock et al.[5] suggested that the Ti assisted the "breaking and re-forming" of covalent Al-H bonds. Several groups performed DFT calculation by substituting Ti into the lattice of the $NaAlH_4$ and Na_3AlH_6 structures. They mostly obtained the lengthening of Al-H bonds by substituting Ti in Na sites. Furthermore, Wang et al.[23] suggested that the interaction between Na-containing and Ti-containing species was crucial. They proposed that the bond between Na^+ and H^- weakened due to the interactions with Ti hydride, and the transfer of H^- from the NaH to AlH_3 was assumed to be an important step in forming covalently bound $[AlH_4]^-$ anions. Very recently, Marashdeh et al.[24] proposed the "zipper" mechanism of Ti catalysis, where the catalytically active Ti species dispersed on the surface of $NaAlH_4$ eject Na ions and other species to the surface, where they can easily react. However, the zipper model only specifically explains the decomposition of alanate; the re-hydrogenation step is assumed to occur by a simple hydrogen pump mechanism.

Quite a number of possible mechanisms for the hydrogen sorption in $MAlH_4$ have been proposed.[25] However, none of these approaches are able to explain the fact that Ti catalyzes both hydrogen desorption steps and the adsorption of hydrogen as perfectly symmetric hysterisis.[1] In this work, we present a completely symmetric mechanism where the function of the catalyst is well-defined. Firstly, we focus exclusively on understanding the main intermediate steps in the dehydrogenation and rehydrogenation of $MAlH_4$ and M_3AlH_6 (where M = Li, Na, and K) based on thermodynamic considerations. With this aim, the Gibbs free energies of each possible compound are calculated from the experimentally available thermodynamic properties of

individual hydrides: $MAlH_4$, M_3AlH_6, and MH. Secondly, the activation barriers of the two extreme cases, that is, no charge separation and complete charge separation, with the intermediates M^+, H^-, MH, and AlH_3, are obtained for the first and second steps. Lastly, we present an atomistic model, based on thermodynamic considerations, where the catalyst acts as a bridge to transfer the MH or M^+ and H^- from AlH_4^- to AlH_6^{3-} and finally to form MH. The proposed mechanism is symmetric and the catalyst forms a bridge between the ions to form transition states M^+---Ti---H^-, MH, and AlH_3 for the (de)hydrogenation.

2. Thermodynamic Analysis

In order to evaluate the reaction path and the activation energies, the thermodynamic stability of the intermediate products of the $MAlH_4$ hydrogen sorption process, the enthalpy of formation and entropy data were collected from the published data and are presented in Table 1. The enthalpy of formation of the elements in the standard state is zero ($H_f^0 = 0$) by definition and the entropy S^0 is determined from the heat capacity at constant volume (C_V). Therefore, for the elements at 298 K, we have $H^0_f = 0$ kJ/mol and S^0_{298}. The Gibbs free energy G° at a temperature T = 298 K is then defined as:

$$G^\circ = H_f{}^\circ - T \cdot S^\circ \tag{4}$$

where H_f° is the enthalpy of formation and S° is the entropy. For any step of the reaction the change in the Gibbs free energy (ΔG) is

$$\Delta G = G_2 - G_1 = H^\circ_{f2} - H^\circ_{f1} - T(S^\circ_2 - S^\circ_1) = \Delta H - T(\Delta S) \tag{5}$$

(remove the f on the right hand side)

Molar heat capacity is a fundamental thermodynamic property that can be measured under constant pressure or volume. These quantities are defined as follows:

$$C_p = \left(\frac{\partial H}{\partial T}\right)_P , \; C_v = \left(\frac{\partial U}{\partial T}\right)_v \tag{6}$$

where H is enthalpy, U is the internal energy, and T is the absolute temperature. The integration of the heat capacity at constant pressure with respect to temperature can be used to calculate the enthalpy and entropy at specific temperature. To obtain the enthalpy and entropy values at 453 K, the following equations are utilized.

$$H_{T_1} = \int_{298}^{T_1} C_p dT + H^\circ \quad (7)$$

$$S_{T_1} = \int_{298}^{T_1} \frac{C_p}{T} dT + S^\circ \quad (8)$$

In Table 1, C_p (T=298 K) values are listed for elements and hydrides. The C_p values of potassium aluminum hydride and hexahydride could not be obtained in the literature. Therefore we estimated C_p (T=298 K) values for $KAlH_4$ and K_3AlH_6 by adding the values of C_p for KH and AlH_3: $C_p(KH)$ = 37.9 J/mol K and $C_p(AlH_3)$ = 40.2 J/mol K (rule of additivity). Bonnetot et al.[43] performed similar calculations for the C_p values of $NaAlH_4$ and Na_3AlH_6. They compared the results obtained from the rule of additivity with experimental C_p values determined by adiabatic calorimetry. In order to verify the data, this rule was also applied for the calculation of the enthalpy of formation and entropy data for the alanates. Satisfactory agreements between estimated and experimental values were obtained except for the enthalpy of formation for Na_3AlH_6. However, with the use of the calculated value of Na_3AlH_6 obtained by the CALPHAD method, the difference between estimated and experimental values was minimized. The higher suitability of the rule of additivity is observed in enthalpy, entropy, and C_p values of hexahydride in our calculations as well as in the calculations of Bonnetot et al., who explained this probable discrepancy by the different surroundings of aluminum atoms in tetra- and hexa-hydridoaluminate. Therefore, we utilized the calculated result of Na_3AlH_6 obtained by the CALPHAD method.

The dissociation energies of the elemental hydrides (LiH = 238.3 kJ/mol,[26] NaH = 205.5 kJ/mol,[27] KH = 176.8 kJ/mol[28]) were used in order to account for the charge transfer in the solid.

$$MH \rightarrow M^{+} + H^{-} \quad (9)$$

The thermodynamics of the hydrogen absorption and desorption reaction can be determined by plotting the plateau pressures and temperatures in a van't Hoff plot.

$$\Delta G = \Delta G^{\circ} + RT \ln \frac{P_{eq}}{P_{eq}^{\circ}} \quad (10)$$

where R is the universal gas constant and P_{eq} is the H_2 equilibrium pressure. At equilibrium, where $\Delta G = 0$, the relationship between H_2 pressure with temperature is given by the Van't Hoff equation as follows:

$$\ln \frac{P_{eq}}{P_{eq}^{\circ}} = -\frac{\Delta H^{\circ}}{R} \cdot \frac{1}{T} + \frac{\Delta S^{\circ}}{R} \quad (11)$$

By plotting ln(p/p°) versus 1/T, the slope is $\Delta H^{\circ}/R$, often remains reasonably constant over the temperature range considered experimentally. The temperature dependence of H_2 sorption pressure between $MAlH_4$ and M_3AlH_6 as well as between M_3AlH_6 and MH was evaluated by utilizing this correlation. The enthalpy difference between the compounds and the elements is called the enthalpy of formation (ΔH_f), while the enthalpy differences between to stable states is called the reaction enthalpy (ΔH_r). Therefore, the enthalpy ΔH^0 in the Van't Hoff equation for the hydrogen desorption is $\Delta H^0 = \Delta H_f$(hexahydride) - ΔH_f(alanate) for the first step and $\Delta H^0 = \Delta H_f$(alkali metal hydride) - ΔH_f(hexahydride) for the second step of the reaction. The standard entropy S^0 of the elements and compounds are given in table 1. The entropy change upon the hydrogen sorption reaction is given by the entropy differences between the standart entropy of the desorbed state plus the standard entropy of hydrogen minus the standard entropy of the hydrides state, therefore, $\Delta S = S^0$(hexahydride) + $S^0(H_2)$ + S^0(aluminum) - S^0(alanate) for the first step and $\Delta S = S^0$(alkali metal hydride) + $S^0(H_2)$ + S^0(aluminum) - S^0(hexahydride) for the second step of the reaction. Since the sum of the standard entropies of the solid products is larger than that of the starting compound in the hydrogen desorption reaction, the resulting entropy change upon the hydrogen desorption is larger than the standard entropy of hydrogen $\Delta S = S^0(M) + S^0(H_2) - S^0(MH)$. This is a major difference to the hydrogen desorption from a metal

hydride, where the standard entropy of the hydride is larger than the standard entropy of the metal and, therefore, the entropy change upon hydrogen desorption is equal or less than the standard entropy of hydrogen gas.

Table 1. Experimental thermodynamic properties of $LiAlH_4$, $NaAlH_4$, and $KAlH_4$ at 298 K at 1 atm.

	$-\Delta H_f^\circ$ (kJ/mol)	Ref	S° (J/mol.K)	Ref	C_p (J/mol.K)	Ref
Al	0	–	28.3	[29]	24.4	[31]
H_2	0	–	130.0	[30]	28.8	[31]
Li	0	–	29.1	[31]	24.8	[31]
Na	0	–	51.2	[31]	28.2	[31]
K	0	–	64.2	[31]	29.6	[31]
LiH	90.6	[32]	20.0	[31]	27.9	[31]
NaH	56.4	[33]	40.0	[31]	36.4	[31]
KH	63.4	[34]	60.7	[35]	37.9	[36]
AlH_3	11.7	[37]	30.0	[37]	40.2	[43]
$LiAlH_4$	115.0	[38]	78.7	[39, 40]	83.2	[31]
$NaAlH_4$	113.0	[35, 41]	89.1	[29, 40]	85.5	[43]
$KAlH_4$	170.5	[42]	112.9	[39]	78.1	–
Li_3AlH_6	311.1	[38]	102.6	[39,31]	127.7	[31]
Na_3AlH_6	238.8[a]	[42]	161.5	[43]	150.6	[43]
K_3AlH_6	308.5	[44]	223.6	[This study][b]	153.9	–

a CALPHAD calculation

b This value was optimized by using two decomposition temperatures acquired from differential thermal analysis in the literature 44

The experimental entropy value for K_3AlH_6 was not available from the literature; therefore in this study these data were calculated based on Equation 5 using experimentally determined temperatures found in the literature[44] for the transition from $KAlH_4$ to hexahydride (T_1) and from hexahydride to KH and Al (T_2) Since the ΔH and ΔS are already known for the hydrogen desorption from $KAlH_4$, the entropy (S°) for K_3AlH_6 was calculated by using two (p,T) pairs acquired from differential thermal analysis in the literature.[44] The calculation details are given in the following section.

3. Results and Discussion

In order to describe the hydrogen sorption reaction of the alkali alanates, for example, $LiAlH_4$, $NaAlH_4$, and $KAlH_4$, the Gibbs free energy along the reaction coordinate was calculated at various temperatures. The Gibbs free energy diagrams were constructed based on

thermodynamic parameters (H_f, S°) as shown in Table 1. $MAlH_4$ (where M = Li, Na, and K) is known to release hydrogen in two distinct steps; partially dehydrogenated M_3AlH_6 and MH phases appear in the dehydrogenation process as indicated in the reaction (1).[4,41] From an atomistic point of view, in the case of $NaAlH_4$, the reaction from the alanate $NaAlH_4$ to the hexahydride Na_3AlH_6 involves the transfer of two NaH to the neighboring $NaAlH_4$ (12):

$$3\ NaAlH_4 \rightarrow AlH_3{\cdot}NaH{\cdots}NaAlH_4{\cdots}NaH{\cdot}AlH_3 \rightarrow Na_3AlH_6 + 2\ AlH_3 \quad (12)$$

$$\rightarrow 3NaH + 3AlH_3 \quad (13)$$

$$\text{in parallel: } AlH_3 \rightarrow Al + {}^3/_2H_2 \quad (14)$$

The second step of the reaction involves the formation of NaH phase from the hexahydride (13). In parallel the alane (AlH_3) decomposes and releases hydrogen (14). Therefore, all possible intermediates in the (de)hydrogenation processes were considered. Only the intermediates among the possible steps that were energetically favorable and preserved the reaction balance to react three moles of $MAlH_4$ were taken into account. The study is based on the experimentally observed intermediates which were already emphasized in the literature for the (de)hydrogenation reactions of $MAlH_4$. In between products transition states, without charge separation (minimum) and with complete charge separation (maximum), are introduced to form the activation barrier in Figure 1 for $LiAlH_4$, Figure 2 for $NaAlH_4$, and Figure 3 for $KAlH_4$.

The calculated Gibbs free energy levels for three moles of $LiAlH_4$ at 453 K are shown in Figure 1. $LiAlH_4$ is stable with respect to the decomposition into elements and thermodynamically unstable with respect to the decomposition with the formation of Li_3AlH_6, Al, and H_2. According to the obtained energy values, the (de)hydrogenation reactions are attributed to two possible reaction pathways including the transition state M^+ and H^- (MAX, complete charge separation) and bonded structure of MH (MIN, no charge separation). The reaction route that connects $LiAlH_4$ to Li_3AlH_6 occurs through a two-step mechanism as shown in Figure 1. First, two $LiAlH_4$ molecules transfer LiH or Li^+ and H^- from each side to the central $LiAlH_4$ and two AlH_3 remain. Secondly, the hexahydride Li_3AlH_6 is formed, the two AlH_3 spontaneously desorb hydrogen, and two Al are left. The experimentally determined activation energy for the transformation of $LiAlH_4$ to Li_3AlH_6 is 111 kJ/mol[45]. This value is in between the levels of the MIN value for the transition state species LiH and the MAX value for Li^+ and H^-

(Figure 1). Since the experimental activation energy is much closer to the MAX level, the transition state is close to the complete charge separation, Li^+ and H^-. The next step is the spontaneous hydrogen desorption from the two AlH_3 to give two Al and three H_2. Kang et al.[46] performed a computational study on the intermediate products for the hydrogen desorption from $LiAlH_4$. In their study, they report the stepwise mechanism involving two sequential hydrogen transfers in the first decomposition reaction of $LiAlH_4$. As a result of these transfers, Li_3AlH_6 plus two AlH_3 molecules are also formed. The driving force for the first reaction step is the thermodynamic stability of the hexahydride. The two Li-H are transferred because the hexahydride is more stable than the alanate; therefore, the movement of the two Li-H has to take place simultaneously.

In the second dehydrogenation step, three LiH are formed from Li_3AlH_6, leaving AlH_3. The reaction proceeds by transferring three hydrogen anions (H^-) from the hexahydride to the lithium cation (Li^+), and three LiH are formed. The two activation energies are 15.6 kJ/mol for the transition state of LiH and 174.4 kJ/mol for Li^+ and H^-. The experimentally determined activation energy for this step is equal to 100 kJ/mol.[45] Here the transition state is closer to the LiH than the separated charges. The reaction of $LiAlH_4$ to form Li_3AlH_6 is exothermic with ΔH_{453} = –35.9 kJ/mol and ΔG_{453} = –36.1 kJ/mol, indicating a spontaneous hydrogen desorption reaction. The Gibbs free energy, ΔG_{298} = –19.8 kJ/mol, is in close agreement with the results of Dymova et al., ΔG_{298} = 27.7 kJ/mol.[47] The direct hydrogen desorption from $LiAlH_4$ to the final product has a higher activation energy as compared to the reaction path via the hexahydride. Therefore, this direct dehydrogenation is not observed.

-Figure 1-

The transition states for the dehydrogenation of $NaAlH_4$ correspond in view of composition to the transition states mentioned above (Figure 2). Therefore the mechanism can be generalized: In both reaction steps of the hydrogen desorption from the alanate the alkali hydride has to move. In the first step two alkali hydrides are transferred to the central alanate in order to form the hexahydride and in the second step three alkali hydrides are removed from the hexahydride. The driving force is the energy gain of the system obtained by forming the

hexahydride and finally the separated alkali hydrides. The hydrogen desorption from the alane is spontaneous. AlH_3 has not been detected experimentally; the reason could be attributed to the unstable behavior of AlH_3, which decomposes immediately into Al and hydrogen at temperatures higher than 418 K.[48] Here the results indicate that the decomposition of AlH_3 is energetically favorable and its formation is likely in order to obtain elemental compounds. At the end of the first decomposition reaction, AlH_3 is responsible for the release of hydrogen. The experimentally reported activation energies of the first and second hydrogen desorption reactions for $NaAlH_4$ are 118 and 124 kJ/mol.[4] The activation barriers for the transition of $NaAlH_4$ to Na_3AlH_6 are 35.9 for NaH and 172.3 kJ/mol for Na^+ and H^-, per formula unit. Therefore, the transition state is in between NaH and Na^+ and H^-, indicating that the real transition state has only partial charge separation.

In the second reaction step, the experimentally determined activation energy is closer to the level of NaH rather than the separated charges Na^+ and H^- for the hydrogen desorption reaction from Na_3AlH_6 to NaH, Al, and H_2. The second reaction step comprises only one transition state: NaH and AlH_3 (Figure 2). Walters and Scogin et al.[49] proposed a similar reaction path in which both $NaAlH_4$ and Na_3AlH_6 release hydrogen by the formation of NaH and AlH_3 as intermediate products. They investigated X-ray diffraction (XRD) patterns, as well as the measured relative composition of selected decomposition samples at various extents of reaction. From those patterns, it was observed that with decreasing concentration of $NaAlH_4$, aluminum metal appears and the concentration of the intermediate Na_2AlH_5 first increases and then decreases when Na_3AlH_6 increases during the progress of the reaction. Furthermore, they suggested that the AlH_3 plays a major role in both the decomposition and the reformation mechanism and they defined the role of Ti as a catalyst center for the formation of Ti–Al alloys, facilitating the AlH_3 formation and sorption for both decomposition and reformation mechanisms. However, the decomposition of AlH_3 is spontaneous and might not need catalysis in order to release hydrogen.

-Figure 2-

At 453 K the most stable phase is $KAlH_4$, as shown in Figure 3, while the most stable phase at that temperature is the elemental hydrides for the $LiAlH_4$ and $NaAlH_4$ system (Figures 1 and 2). The Gibbs free energies of $LiAlH_4$ and $NaAlH_4$ are similar, while that of $KAlH_4$ is 67 kJ/mol lower than that of $NaAlH_4$. This is because in the reaction $MAlH_4 \rightarrow MH + Al + 3/2\ H_2$, the enthalpy change with M = K is more endothermic than that with M = Na. Therefore a higher decomposition temperature is required for $KAlH_4$ (573–673 K) as compared to $NaAlH_4$ under ambient H_2 pressure. The (de)hydrogenation steps for $KAlH_4$ follow the same reaction path as in the cases of $LiAlH_4$ and $NaAlH_4$. Ares et al.[44] reported that the apparent activation energies are 131 and 140 kJ/mol for the first and second decompositions of $KAlH_4$. The experimentally obtained activation energy values from the literature and the calculated values in this study for the two main decomposition steps of Li, Na, and K alanates reveal that both activation barriers tend to be higher when the alkaline metal is larger or less electronegative. They are in the following order: $LiAlH_4 < NaAlH_4 < KAlH_4$. The higher activation barriers found for the hydrogen desorption in $KAlH_4$ can be explained by the more pronounced charge separation in the transition state for the less electronegative alkali metals.

-Figure 3-

The Gibbs free energy of the alanate and the hexahydride determine the thermodynamic stability of compounds and also their temperature of hydrogen release at 1 bar pressure. In Figure 4, the Gibbs free energy values for the selected levels are shown at different temperatures. The values are calculated by varying temperatures between 290 and 400 K for $NaAlH_4$ and 590 and 630 K for $KAlH_4$. The temperatures for the transition from $MAlH_4$ to hexahydride (T_1) and from hexahydride to MH and Al species (T_2) are denoted by T_1 and T_2. Those values are calculated where the difference between the Gibbs free energy level of $MAlH_4$ and M_3AlH_6, or M_3AlH_6 and MH is zero by utilizing equation of $\Delta G = \Delta H - T\Delta S$. The calculated values for $NaAlH_4$ are 295 and 382 K. The temperature dependences of hydrogen desorption from $MAlH_4$ to M_3AlH_6 as well as from M_3AlH_6 to MH are shown in Figure 4, where the Gibbs free energy is plotted over the reaction coordinate at several temperatures. Bogdonavic et al.[50] experimentally determined the van't Hoff plot of the dissociation pressures of the hydrogen desorption from $NaAlH_4$ and

Na_3AlH_6. For the two-step reversible hydrogen sorption of the Ti-doped $NaAlH_4$, the hydrogen pressures for $NaAlH_4$ at 456 K and for Na_3AlH_6 at 517 K are 135 and 64 bar, respectively.[50] The extrapolated hydrogen dissociation pressures at 1 bar for $NaAlH_4$ and Na_3AlH_6 are found at 292 and 377 K, respectively, which is in excellent agreement with the equilibrium conditions in the Gibbs free energy diagrams.

The experimental entropy value for K_3AlH_6 was not available from the literature; therefore the data were calculated by considering the experimentally found equilibrium temperatures T_1 and T_2. Ares et al.[44] investigated the thermal hydrogen desorption of the as-prepared $KAlH_4$ by means of a differential thermal analyzer at 1 atm. This study confirmed that the desorption reaction path is a multistep dehydrogenation. They found that $3KAlH_4$ undergoes an initial decomposition reaction to form $K_3AlH_6 + 2AlH_3$ at 593 K and a second decomposition of K_3AlH_6 into $3KH + 2AlH_3$ at 628 K. Those two temperatures were used in order to calculate the standard entropy of K_3AlH_6. The entropy was determined by equating two energy levels of the decomposition phases, that is, transition from $KAlH_4$ to K_3AlH_6 and from K_3AlH_6 to KH (Figure 4). The optimized entropy for K_3AlH_6 is about 223.6 J/mol K. The obtained entropy value of K_3AlH_6 confirms the Gibbs free energy analysis, as the entropy of K_3AlH_6 is lower than those of Na_3AlH_6 and Li_3AlH_6. In addition to that, starting from the values of S° for KH and AlH_3 ($S^\circ(KH)$ = 60.7 J/ mol K and $S^\circ(AlH_3)$ = 30 J /mol K) and using the rule of additivity, we achieved the estimated S° value for K_3AlH_6: 212.1 J /mol K. This is very close to the value obtained by equating the two energy levels of the decomposition phases in this study.

-Figure 4-

In spite of the difference in their crystal structures, the types of decomposition products, that is, the reaction pathways, for the three alkali alanates under investigation are all the same. This indicates that the mechanism for all three alanates may be similar. A large variety of possible mechanisms for the Ti-catalyzed hydrogen sorption in $MAlH_4$ have been proposed.[25] However, the decomposition of both $MAlH_4$ and M_3AlH_6 and the rehydrogenation of the solid decomposition products in the presence of Ti were not fully explained. In Figure 5, we illustrate a completely symmetric mechanism where the catalyst has a well-defined function in each reaction step, that is, to form a bridge between the ions $M^+\cdots Ti\cdots H^-$ and therefore avoid a

complete charge separation. Specifically considering the alanates, the transition states, the hexahydride, and the elemental hydrides, the role of Ti is clarified. As shown by the Gibbs free energy diagrams, the hydrogen sorption mechanism for $MAlH_4$ follows a reaction pathway in between M^+ and H^- (MAX, complete charge separation) and MH (MIN, no charge separation) along with AlH_3 in both hydrogen (de)adsorption reactions. Furthermore, Figure 5 illustrates that Ti acts as a bridging atom for the ion transfer: Ti bridges two H^- and M^+ from two $[AlH_4]^-$ to the neighboring $MAlH_4$ in the first step and Ti bridges three H^- and M^+ from the Na_3AlH_6 to form NaH in the second step. During the decomposition of Na_3AlH_6, three H^- and M^+ are produced by the removal of three NaH in a side-reaction. At this point, the presence of Ti facilitates the rapid decomposition of Na_3AlH_6, with the possibility of forming TiH^-. Sc, V, Ce, and Pr, which also work as fairly effective catalysts in alanates, are able to form analogous hydride structures.

The role of Ti in the catalyzed rehydrogenation reaction follows the same path as the dehydrogenation steps. This symmetrical reaction path might also be the reason why the isotherm of the reabsorption follows the desorption isotherm with almost no hysteresis according to the pressure–composition–temperature (PCT) analysis.[1,5,6] In order to initiate rehydrogenation, conditions that allow the formation of AlH_3 from Al are necessary. While the decomposition reaction of AlH_3 occurs spontaneously, the formation of AlH_3 from Al requires hydrogen at high pressure. Graetz et al.[51] performed *ab initio* calculations of the free energy, showing that the minimum H_2 pressure necessary for AlH_3 hydride formation at 300 K is 700 MPa (fugacity of H_2 = 50 GPa). This is in agreement with high-pressure hydrogenation experiments.[52] The equilibrium reaction $Al + {}^3/_2H_2 \leftrightharpoons AlH_3$ is pressure dependent. During the rehydrogenation, the formation of AlH_3 depends on the left hand side reaction by requiring high hydrogen pressure. However, even high pressure is required and also even a desired product is not thermodynamically favored for the AlH_3 formation, the AlH_3 can be obtained if it is continuously removed from the reaction. Since the formed AlH_3 is immediately consumed in the catalyzed (Ti) subsequent step together with NaH to form the hexahydride or the alanate, the reaction continues to produce AlH_3 by proceeding from left to right. In other words, the concentration of AlH_3 is decreasing in the system because it is consumed to produce both of the alanates, first Na_3AlH_6 and then $NaAlH_4$. Here Ti is important to form bridge between M+ and H^-, which is then combined with AlH_3 to form hexahydride and alanate. The reason of requiring much higher pressure for pure AlH_3 may be related to the presence of many unreacted AlH_3 in

the system. In the case of $NaAlH_4$ and $KAlH_4$, the required pressure value for the formation of AlH_3 can be lower due to the presence of M+ and H^- that decrease concentration of AlH_3 in the system. This is a different scenario from that proposed by Bogdanovic, where seemingly metallic aluminum particles react with NaH to form Na_3AlH_6. Bogdanovic et al.[53] further indicated that adding extra aluminum provides a complete reformation of $NaAlH_4$. According to our proposed mechanism, adding extra aluminum to the system may also promote the formation of additional AlH_3, which interacts with NaH to form Na_3AlH_6 and then $NaAlH_4$.

-Figure 5-

Sandrock et al.[5] report that Ti aids the breaking and reforming of covalent Al-H bonds by lowering the activation energy for that process. They also showed that the activation energies for the decomposition of the $NaAlH_4$ and Na_3AlH_6 drop to much lower and different levels when even a small amount of catalyst is added (0.9%). With further addition of $TiCl_3$ to the system, the activation energy remains virtually constant, indicating that there is no further change in the fundamental mechanism. In another study conducted by Sandrock et al.,[54] the positive effect of Ti together with LiH on desorption rates in contrast to the addition of only Ti to AlH_3 is discussed. This may indicate the beneficial interactions of Ti atoms with M^+ and H^-, which are essential to form hexahydride and the elemental hydride structure. Since AlH_3 species are very unstable and decompose spontaneously, those species could not be observed at the end of the first and second decomposition steps. The immediate decomposition may be the reason why they are not yet experimentally observed. However, the possibility of their presence cannot be ignored.

4. Conclusions

The Gibbs free energy diagrams were constructed in order to determine the stability of intermediates, products, and reactants based on the published experimental thermodynamic data. We restricted the intermediates among the energetically favorable steps, conserving the reaction balance of three moles of $MAlH_4$. All investigated alkali alanates follow the same hydrogen desorption mechanism, where the hexahydride is formed by transferring the alkali cation and a

hydrogen anion from the two neighboring alanates to the central one, which forms the hexahydride. The activation energy of the transfer of an alkali hydride MH is lower than the experimentally determined activation energy, while the transfer of M^+ and H^- is energetically above the experimental value. Therefore, the degree of charge separation determines the activation energy. The role of the Ti catalyst is to reduce the charge separation by forming a bridge between the M^+ and the H^-. The second reaction step again involves the movement of the alkali hydride. Again the Ti plays the same role of forming a bridge. The standard entropy of K_3AlH_6 was estimated to be 223.6 J/mol.

References

1 B. Bogdanovic, M. Schwickardi, *J. Alloys Compd.,* 1997, **253–254**, 1–9.

2 M. Pozzo, D. Alfe, *Int. J. Hydrogen Energy,* 2011, **36**, 15632–15641.

3 V. P. Balema, L. Balema, *Phys. Chem. Chem. Phys.,* 2005, **7**, 1310–1314.

4 B. Bogdanovic, G. Sandrock, *MRS Bull. Sept.,* 2002, **27**, 712–716.

5 G. Sandrock, K.Gross, Thomas. G. *J. Alloys Compd.,* 2002, **339**, 299–308.

6 W. Luo, K. Gross, J. *J. Alloys Compd.,* 2004, **385**, 224–231.

7 A. Leon, O. Kircher, M. Fichtner, J. Rothe, D. Schild, *J. Phys. Chem., B*., 2006, **110**, 1192-1200.

8 H. W. Brinks, M. Sulic, C. M. Jensen, B. C. Hauback, *J. Phys.Chem. B.,* 2006, **110**, 2740–2745.

9 M. P. Pitt, P. E. Vullum, M. H. Sørby, M. P. Sulic, C. M. Jensen, J. C. Walmsley, R. Holmestad, B. C. Hauback, *Acta Mater.,* 2008, **56**, 4691–4701.

10 P. Wang, X. D. Kang, H. M. Cheng, *Chem. Phys. Chem*., 2005, **6**, 2488–2491.

11 C. P. Balde, A. M. J. van der Eerden, H. A. Stil, F. M. F. de Groot,K. P. de Jong, J. H. Bitter, J. *Alloys Compd.,* 2007, **446–447**, 232–236.

12 G. J. Lee, J.-H. Shim, Y. W. Cho, K. S. Lee, *Int. J. Hydrogen Energy*, 2008, **33**, 3748–3753.

13 K. J. Gross, E. H. Majzoub, S. W. Spangler, *J. Alloys Compd.,* 2003, **356–357**, 423–428.

14 C. M. Jensen, R. Zidan, N. Mariel, A. Hee, H. Chrystel, *Int. J. Hydrogen Energy,* 1999, **24**, 461-465.

15 B. Bogdanović, M. Felderhoff, A. Pommerin, F. Schüth, N. Spielkamp, *Adv. Mater.,*

2006, **18**, 1198–1201.

16 T. Wang, J. Wang, A. D. Ebner, J. A. Ritter, *J. Alloys Compd.,* 2006, **450**, 293–300.

17 E. Ivanov, I. Konstanchuk, A. Stepanov, V. Boldyrev, *J. Less-Common Met.,* 1987, **131**, 25–29.

18 H. Gunaydin, K. N. Houk, V. Ozolins, *Proc. Natl. Acad. Sci.,* 2008, **105**, 3673-3677.

19 A. Borgschulte, A. Zuttel, P. Hug, G. Barkhordarian, N. Eigen, M. Dornheim, R. Bormann, A. Ramirez-Cuesta, *J. Phys. Chem. Chem. Phys*., 2008, **1**, 4045-4055.

20 A. Peles, C. G. van de Walle, *Phys. Rev. B.,* **2007**, 76, 214101.

21 D. Sun, S. S. Srinivasan, G. Chen, C. M. Jensen, *J. Alloys Compd.,* 2004, **373**, 265.

22 S. Singh, S. W. H. Eijt, J. Huot, W. A. Kockelmann, M. Wagemaker, F. M. Mulder, *Acta Mater.,* 2007, **55**, 5549-5557.

23 P. Wang, X. D. Kang, H. M. Cheng, *J. Phys. Chem. B.* 2005, **109**, 20131.

24 A. Marashdeh, R. A. Olsen, O. M. Løvvik, G. J. Kroes, *J. Phys. Chem. C.,* 2008, **112**, 15759–15764.

25 T. J. Frankcombe, *Chem. Rev.,* 2012, **112**, 2164–2178.

26 K. Kenneth, Modern Physics, 2nd ed.; Wiley, 1996.

27 N. Sreedhara Murthy, T. Manisekaran, N.S. Bapat, *Quant J. Spectrosc. Radiat. Transf.,* 1983, **29**, 183–187.

28 F. Qun-Chao, W. G. Sun, *Chin. Phys. Lett.,* 2008, **25**, 2012–2015.

29 D. R. Lide, Ed., CRC Handbook of Chemistry and Physics, 80th ed.; CRC Press: Boca Raton, 2000.

30 D. J. Siegel, C. Wolverton, V. Ozoliņš, *Phys. Rev. B*, 2007, **76**, 134102.

31 D. D. Wagman, W. H. Evans, V. B. Parker, R. H. Schumm, R. L. Nuttall, Selected values of chemical thermodynamic properties [Part 8]. Compounds of Uranium, Protactinium, Thorium, Actinium, and the Alkali Metals, Volume: NBS Technical Note 270-8; National Bureau of Standards, 1981.

32 A. J. Bard, R. Parsons, J. Jordan, Standard Potentials in Aqueous Solution; New York, 1985.

33 S. R. Gunn, L. G. Green, *J. Am. Chem. Soc.,* 1958, **80**, 4782-4786.

34 J. Sangster, A. D. Pelton, *J. Phase Equilib.,* 1997, **18**, 387–389.

[35] M. B. Smith, Jr. G. E. Bass, *J. Chem. Eng. Data,* 1963, **8**, 342-346.

[36] M.W. Jr. Chase, NIST-JANAF Themochemical Tables, 4th ed., *J. Phys. Chem. Ref. Data Monograph,* 1998, 9, 1–1951.

[37] G. C. Sinke, L. C. Walker, F. L. Oetting, D. R. Stull, *J. Chem. Phys.,* 1967, **47**, 2759-2761.

[38] P. Claudy, B. Bonnetot, J. M. Letoffe, G. Turck, *Thermochim. Acta,* 1978, **27**, 213–221.

[39] Gavrichev, K. S. *Inorg. Mater.* **2003**, 39, 89–112.

[40] B. Bonnetot, P. Claudy, M. Diot, J. M. Létoffé, *J. Chem. Thermodyn.,* 1979, **11**, 1197–1202.

[41] S.-I. Orimo, Y. Nakamori, J. R. Eliseo, A. Züttel, C. M. Jensen, *Chem. Rev.,* 2007, **107**, 4111–4132.

[42] T. N. Dymova, D. P. Aleksandrov, V. N. Konoplev, T. A. Silina, N. T. Kuznetsov, *Russ. J. Coord. Chem. C/C of Koordinatsionnaia Khimiia,* 1993, **19**, 529–534.

[43] B. Bonnetot, G. Chahine, P. Claudy, M. Diot, J. M. Letoffe, *J. Chem. Thermodyn.,* 1980, **12**, 249–254.

[44] J. R. Ares, K.-F. Aguey-Zinsou, F. Leardini, I. Jimenez Ferrer, J.F. Fernandez, Z.-X. Guo, C. Sanchez, *J. Phys. Chem. C,* 2009**, 113**, 6845–6851.

[45] R.A. Varin, L. Zbroniec, *J. Alloys Compd.,* 2010, **504**, 89–101.

[46] J. K. Kang, J.Y. Lee, R. P. Muller, W. A. Goddard, III. *J. Chem. Phys.,* 2004, **121**, 10623.

[47] T. N. Dymova, D. P. Aleksandrov, V. N. Konoplev, T. A. Silina, A. S.Sizareva, *Russ. J. Coord. Chem.,* 1994, **20**, 279-285.

[48] J. Graetz, J. J. Reilly, *J. Phys. Chem. B*, 2005, ***109***, 22181–22185.

[49] R.T. Walters, J.H. Scogin, *J. Alloys Compd*.,2004, **379**, 135-142.

[50] B. Bogdanovic, R.A. Brand, A. Marjanovic, M. Schwickardi, J. Tolle, *J. Alloys Comp.,* 2000, **302**, 36–58.

[51] J. Graetz, S. Chaudhuri, Y. Lee, T. Vogt, J. T. Muckerman, J. Reilly, *J. Phys. Rev. B,* 2006, **74**, 214114

[52] A. K. Konovalov, B. M. Bulychev, *Inorg. Chem.,* 1995, **34**, 172-175.

[53] B. Bogdanovic, M. Felderhoff, M. Germann, M. Hartel, A. Pommerin, F. Sschuth, C. Weidenthaler, B. Zibrowius, *J. Alloys Compd.*, 2003, **350**, 246–255.

[54] G. Sandrock, J. Reilly, J. Graetz, W.M. Zhou, J. Johnson, J. Wegrzyn, *Appl. Phys. A,*

2005, **80**, 687-690.

Figure Captions

Fig.1 Gibbs free energy diagram of the hydrogen sorption reaction in $LiAlH_4$ and the intermediates formed at 453 K. The levels of the minimum reaction path (no charge separation) in blue (-), the levels based on the experimentally found activation energies in orange (-), and the maximum reaction path (complete charge separation) in red (-) are shown.

Fig. 2 Gibbs free energy diagram of the hydrogen sorption reaction in $NaAlH_4$ and the intermediates formed at 453 K. The levels of the minimum reaction path (no charge separation) in blue (-), the levels based on the experimentally found activation energies in orange (-), and the maximum reaction path (complete charge separation) in red (-) are shown.

Fig. 3 Gibbs free energy diagram of the hydrogen sorption reaction in $KAlH_4$ and the intermediates formed at 453 K. The levels of the minimum reaction path (no charge separation) in blue (-), the levels based on the experimentally found activation energies in orange (-), and the maximum reaction path (complete charge separation) in red (-) are shown.

Fig. 4 Transition temperatures for the reactions from $MAlH_4$ to hexahydride (T_1) and from hexahydride to MH and Al species (T_2) and the temperatures in between these transitions (T_{1-2}) for **(a)** $NaAlH_4$ and **(b)** $KAlH_4$.

Fig. 5 The function of the Ti is to bridge H^- and M^+ (M^+---Ti---H^-) in order to remove the ion couple from the $MAlH_4$ or M_3AlH_6 without the need to transfer individual M^+ and H^- ions.

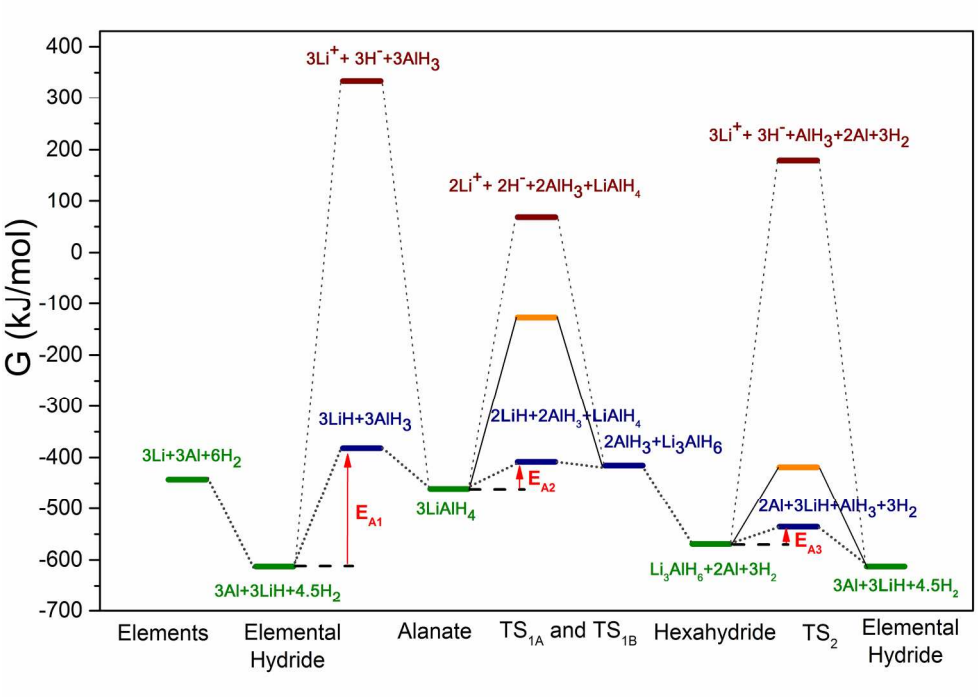

Fig.1 Gibbs free energy diagram of the hydrogen sorption reaction in LiAlH4 and the intermediates formed at 453 K. The levels of the minimum reaction path (no charge separation) in blue (-), the levels based on the experimentally found activation energies in orange (-), and the maximum reaction path (complete charge separation) in red (-) are shown.
201x141mm (300 x 300 DPI)

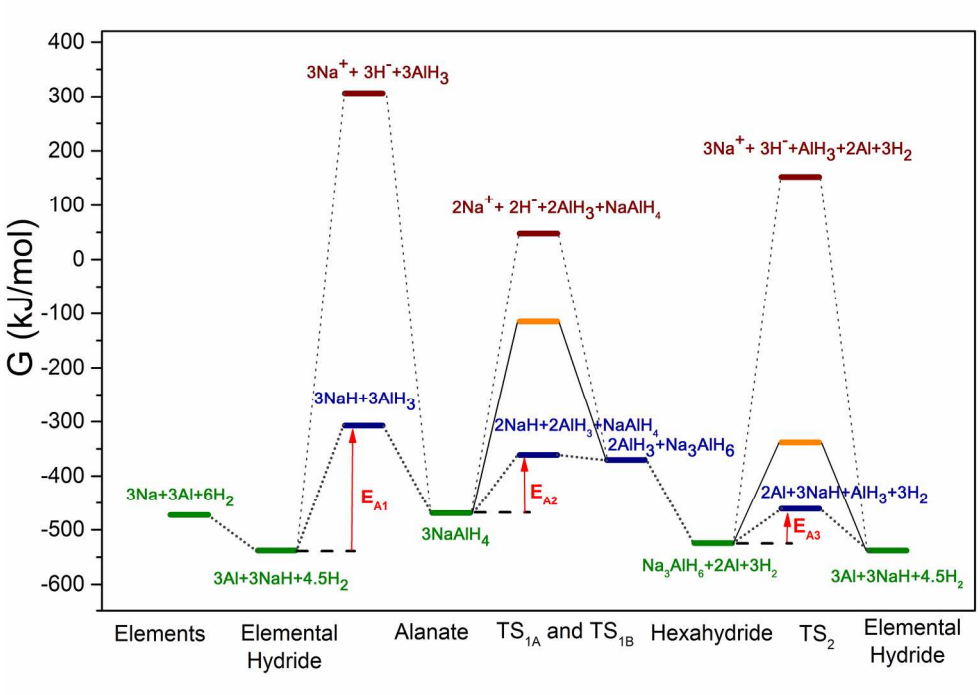

Fig. 2 Gibbs free energy diagram of the hydrogen sorption reaction in NaAlH4 and the intermediates formed at 453 K. The levels of the minimum reaction path (no charge separation) in blue (-), the levels based on the experimentally found activation energies in orange (-), and the maximum reaction path (complete charge separation) in red (-) are shown.
201x141mm (300 x 300 DPI)

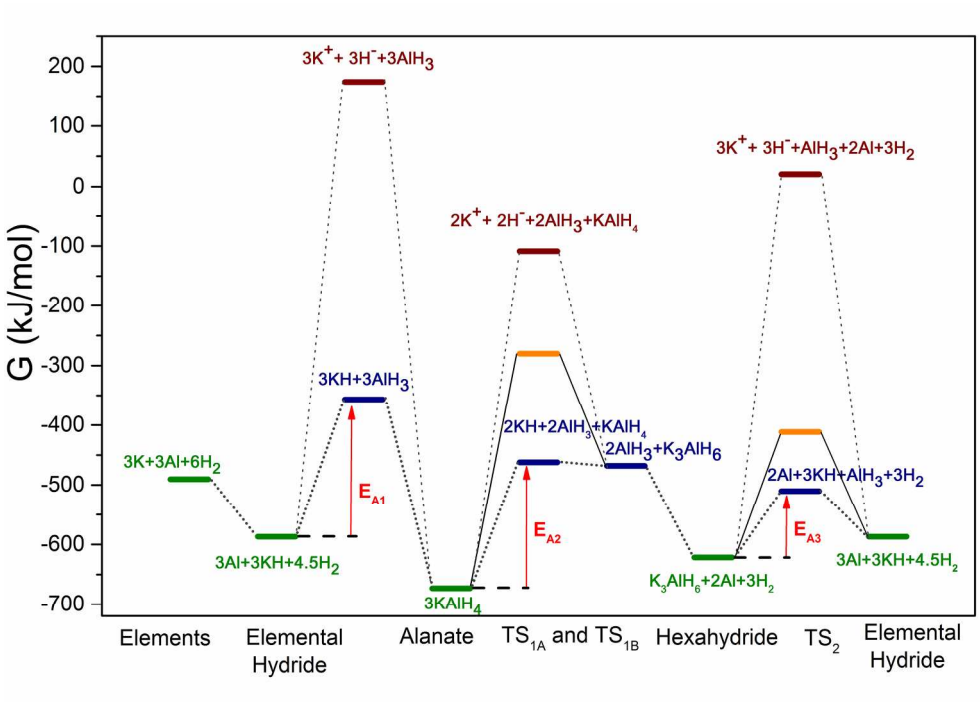

Fig. 3 Gibbs free energy diagram of the hydrogen sorption reaction in KAlH4 and the intermediates formed at 453 K. The levels of the minimum reaction path (no charge separation) in blue (-), the levels based on the experimentally found activation energies in orange (-), and the maximum reaction path (complete charge separation) in red (-) are shown.
201x141mm (300 x 300 DPI)

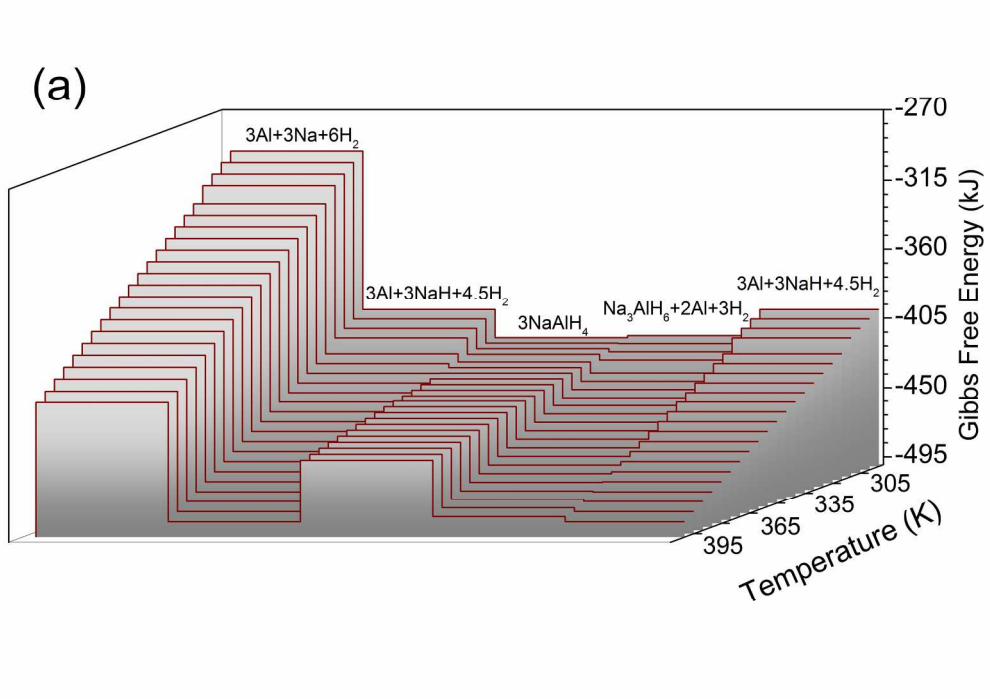

Fig. 4 Transition temperatures for the reactions from MAlH4 to hexahydride (T1) and from hexahydride to MH and Al species (T2) and the temperatures in between these transitions (T1–2) for NaAlH4
201x141mm (300 x 300 DPI)

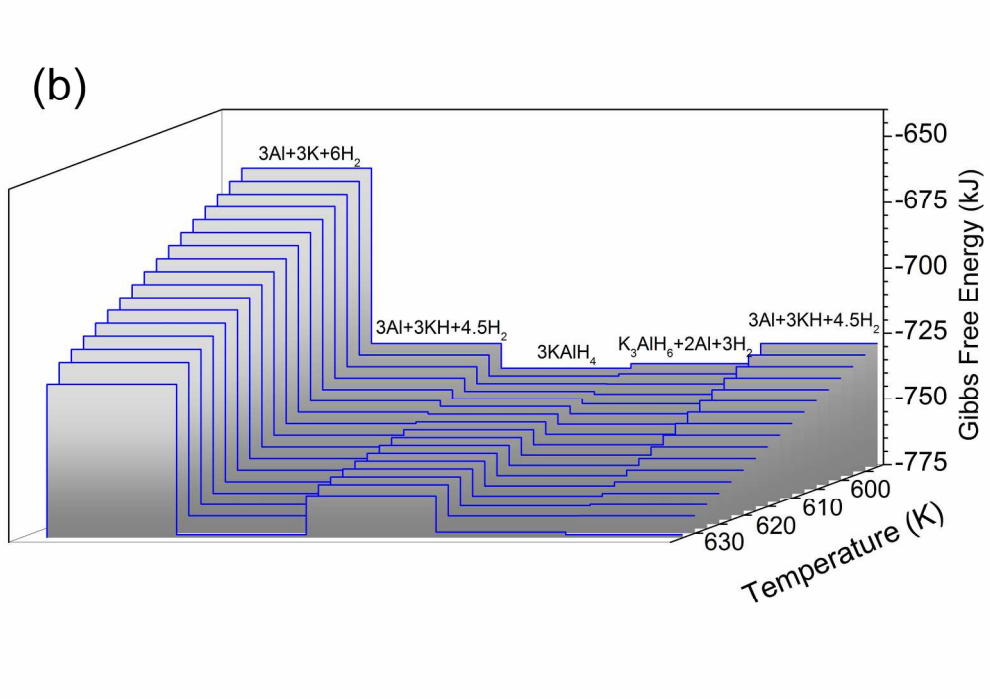

Fig. 4 Transition temperatures for the reactions from MAlH4 to hexahydride (T1) and from hexahydride to MH and Al species (T2) and the temperatures in between these transitions (T1–2) for KAlH4.
201x141mm (300 x 300 DPI)

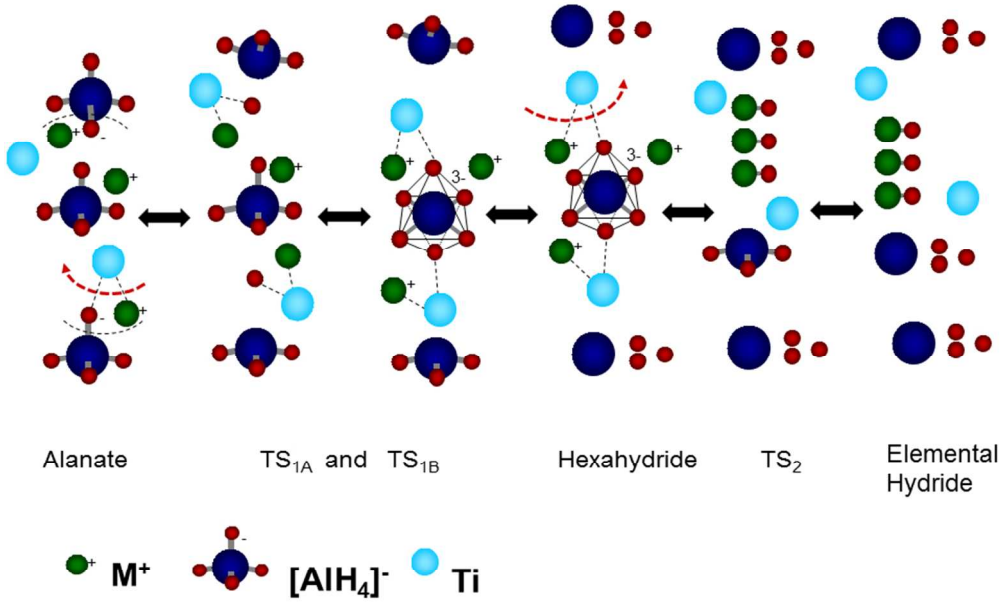

Fig. 5 The function of the Ti is to bridge H- and M+ (M+---Ti---H-) in order to remove the ion couple from the MAlH4 or M3AlH6 without the need to transfer individual M+ and H- ions.
254x190mm (96 x 96 DPI)